Geophysical Journal International

Geophys. J. Int. (2010) **180,** 34–48 doi: 10.1111/j.1365-246X.2009.04401.x

Seismic reflection character of the Hikurangi subduction interface, New Zealand, in the region of repeated Gisborne slow slip events

Rebecca Bell, Rupert Sutherland, Daniel H. N. Barker, Stuart Henrys, Stephen Bannister, Laura Wallace and John Beavan

GNS Science, 1 *Fairway Drive, Avalon, Lower Hutt* 5010*, New Zealand. E-mail: R.Bell@gns.cri.nz*

Accepted 2009 September 28. Received 2009 September 27; in original form 2009 March 3

SUMMARY

We use seismic reflection data to map the geometry and character of the subduction interface in the Gisborne area of the Hikurangi subduction margin, New Zealand, which experiences repeated shallow (<15 km) slow slip events. The reflection character and geometry in this area is highly variable, which we interpret to be related to the subduction of seamounts and underthrust sediments. Three zones of high-amplitude interface reflectivity (HRZ-1, 2 and 3) are interpreted to be the result of fluid-rich sediments that have been entrained with subducting seamounts. The interface above the HRZ zones is shallower than the surrounding areas by 2–4 km, due to the warping of the interface to accommodate seamount subduction. These zones of high-amplitude reflectivity and shallower interface geometry correlate broadly with locations of recorded slow slip events from 2002 to 2008. We hypothesize that effective stresses on the interface may be lower along the northeast margin in areas of high-amplitude reflectivity due to; (1) the enhanced underthrusting of fluid-rich sediment, (2) reduced overburden stresses where the interface has been warped to shallower depths to accommodate seamount subduction and (3) potential fluid flow concentration effects leading to overpressure along these shallower interface corrugations. From our observations we propose localized reductions in effective stress caused by interface structural relief may be a potential factor in promoting shallow slow slip events.

Key words: Transient deformation; Controlled source seismology; Seismicity and tectonics; Subduction zone processes.

1 INTRODUCTION

Slow slip events, or 'silent earthquakes' with much longer rupture times than ordinary earthquakes, and which result in crustal movements with velocities 1–100 times background tectonic levels, have been detected at many Pacific Rim subduction margins (e.g. Dragert *et al.* 2001; Ozawa *et al.* 2001; Hirose & Obara 2005; Obara & Hirose 2006; Wallace & Beavan 2006; Schwartz & Rokosky 2007). The moment release of slow slip events over many days or months if released as a single event is often of the order $M_w = 6$–7 (e.g. Dragert *et al.* 2001; Wallace & Beavan 2006). Slow slip events could therefore play an important role in cumulative stress loading of the shallower seismogenic zone, increasing the possibility of triggering failure in the locked zone (e.g. Linde & Silver 1989) or slow slip itself may be triggered by large earthquakes (as speculated in Francois-Holden *et al.* 2008).

The mechanism for slow slip initiation is still poorly understood, but thought to be related to the transition between velocity-strengthening and velocity-weakening behaviour (e.g. Scholz 1998; Shibazaki & Iio 2003; Yoshida & Kato 2003; Lowry 2006; Liu & Rice 2007; Schwartz & Rokosky 2007; Rubin 2008). Laboratory experiments have shown that short-period transient displacements can occur spontaneously at this transition zone if effective normal stresses are reduced, which can be achieved by increases in pore pressures or changes in plate geometry (Yoshida & Kato 2003; Mitsui & Hirahara 2006; Liu & Rice 2007). The segmented nature of slow slip patches along margins has been related to changes in plate coupling (Hirose & Obara 2005), changes in subduction geometry (Mitsui & Hirahara 2006) and differences in the strength of subducting and/or overriding geological terrains (Brudzinski & Allen 2007). It has also been associated with subducting asperities (i.e. seamounts and ridges) (Yoshida & Kato 2003; Kodaira *et al.* 2004; Heki & Kataoka 2008).

Seismic tremor accompanying slow slip events at some margins has been related to dehydration reactions, adding further support that fluid is important in inducing slow slip (Obara 2002; Brown *et al.* 2005; Hirose & Obara 2005; McCausland *et al.* 2005; Obara & Hirose 2006; Schwartz & Rokosky 2007). Alternatively, others suggest that tremor can occur on the plate interface coincident with inferred zones of slow slip and is the result of shear slip, possibly assisted by high fluid pressures, rather than fluid flow (Shelly *et al.* 2006).

Slow slip events have been interpreted in areas where the transition between stick-slip and stable sliding behaviour occurs at ∼350 °C (Dragert *et al.* 2001; Kodaira *et al.* 2004; Wallace & Beavan 2006), as well as in regions where the transition is much shallower ∼100–150 °C (Douglas *et al.* 2005; McCaffrey *et al.* 2008). Therefore, temperature may not be the primary control on their occurrence (McCaffrey *et al.* 2008).

Seismic reflection imaging can reveal subduction interface geometry and is effective at highlighting likely fluid-affected areas, and so is potentially an important tool in mapping (in conjunction with geodetic and seismology studies) possible stick-slip versus stable sliding patches on the shallow part of the interface (Nedimovic *et al.* 2003; Sage *et al.* 2006; Ranero *et al.* 2008). For example, high-amplitude reflections define the plate interface of the Costa Rica-Nicaragua margin at depths corresponding to calculated temperatures of 60–150° and are interpreted as being due to the presence of free water along the decollement (Ranero *et al.* 2008).

Active source seismic studies around the Pacific have revealed a number of subduction interface features that may be related to slow slip. Nedimovic *et al.* (2003) and Calvert (2004) have identified at the Cascadia margin a thin band of high-amplitude reflections in what they propose to be the locked unstable zone, and a broader band of high-amplitude reflections in the zone of stable sliding that experiences slow slip. Nedimovic *et al.* (2003) propose that the wide high-amplitude reflection band may represent interlayered metamorphic or sedimentary rocks, or sheared sediments that trap fluids released in the subducting plate. Calvert (2004) conversely proposes that it is the result of a wide megathrust shear zone. A similar increase in the width of the high-amplitude reflection band defining the subduction thrust has been observed at the Alaskan margin (Fisher *et al.* 1989). In addition, a high-amplitude reflectivity zone, interpreted as a zone of high-porosity downdip of a subducting ridge is found to correlate closely with the Tokai slow slip event at the Nankai trough (Kodaira *et al.* 2004). Although no slow slip events have been observed at the Japan Trench, a similar inverse relationship between high-amplitude interface reflections and low levels of seismicity are thought to relate to a low-velocity layer along the Japan Trench interface due to aqueous fluid and/or hydrated rocks (Fujie *et al.* 2002; Mochizuki *et al.* 2005).

Repeated slow slip events have been recorded offshore the Gisborne area of the Hikurangi subduction margin, New Zealand, at shallower depths on the interface (<15 km) than elsewhere in the world. The same area of the interface has also experienced two shallow tsunami earthquakes in 1947. In this contribution, we interpret in detail the geometry and seismic reflection character of the subduction interface that has undergone slow slip offshore Gisborne from a regional grid of 2-D high-resolution seismic reflection profiles. This is a unique data set. At other subduction margins, slow slip events have been recorded no shallower than depths of 20–45 km, which is deeper than the imaging capabilities of high-resolution seismic reflection data. From our structural mapping of interface characteristics, we propose a conceptual model for the occurrence of shallow slow slip along this particular segment of the margin.

2 TECTONIC SETTING AND SLOW SLIP EVENTS IN THE GISBORNE AREA

The Hikurangi subduction margin, along the east coast of the North Island, New Zealand, lies to the south of the Tonga–Kermadec chain and experiences convergence rates between the Pacific Plate and the forearc of ∼60 mm yr^{-1} to the north in an approximately margin-normal orientation, decreasing to <30 mm yr^{-1} of oblique convergence to the south (Fig. 1; Wallace *et al.* 2004). The margin varies significantly along strike in terms of subduction interface seismogenic zone properties and geometry (e.g. Reyners 1998; Wallace *et al.* 2004; Barker *et al.* 2009). According to geodetic models, the subduction interface is locked during the current interseismic period to depths of 30–50 km beneath the southern North Island, whereas interseismic locking only occurs to depths of 10–15 km beneath northeast North Island (Wallace *et al.* 2004). This mirrors a southward increase in depth of the downdip limit of the seismogenically inferred subduction interface seismogenic zone (Reyners 1998). Most of the historic interface rupturing earthquakes have occurred either within the region of weak interseismic coupling to the north, or along the edges of the strongly interseismically coupled portion to the south (Wallace *et al.*, submitted). There are clear differences in the seismogenic behaviour of the north and south Hikurangi margin. Variations in the fluid pressure along the interface and in the hangingwall has been proposed as an explanation for the differing downdip limits of the seismogenic zone (Fagereng & Ellis 2009).

The east coast of the North Island has experienced nine slow slip events recorded by continuous global positioning systems (CGPS) between 2002 and 2008 (Douglas *et al.* 2005; Wallace & Beavan 2006; McCaffrey *et al.* 2008; GNS Science, unpublished data). The ∼1 year duration 2004–2005 Manawatu and 2003–2004 Kapiti events in the southern North Island (Fig. 1a) took place at a depth of 30–50 km near the downdip limit of an area of strong present-day coupling on the subduction interface (Wallace & Beavan 2006). In the Gisborne region (Fig. 1), where the present-day coupling on the interface is shallower and weaker (Reyners 1998; Wallace *et al.* 2004), six slow slip events with durations of around 10 days have occurred between 2002 and 2008 at depths of 10–15 km (Douglas *et al.* 2005; McCaffrey *et al.* 2008). Seismicity during a slow slip event in 2004 has been studied in detail by Delahaye *et al*. (2009), who show that the slow slip event was accompanied by distinct microseismic earthquakes, rather than tremor. The largest rupturing earthquakes identified on the Hikurangi interface using post-1917 teleseismic records (e.g. Webb & Anderson 1998; Doser & Webb 2003) occurred offshore the Gisborne region in March and May 1947 (Doser & Webb 2003). The 1947 earthquakes had characteristics of "tsunami earthquakes" (Kanamori 1972; Fukao 1979; Pelayo & Wiens 1992), including locations close to the trench where the interface is at very shallow depths, slow rupture velocities, long source–time durations, low energy release at high frequencies and larger than expected tsunami (run-ups of 10 and 6 m, respectively) (Downes *et al.* 2000; Doser & Webb 2003).

The slow slipping part of the subduction interface responsible for the 2002 Gisborne event has previously been modelled by Douglas *et al.* (2005) from forward modelling of just two CGPS measured displacements. They argued that the downdip limit was well constrained at ∼15 km deep, ∼20 km east of Gisborne, although the updip limit and along-strike length are poorly constrained (resolution of along-strike length is improved for later events due to extra CGPS sites; e.g. McCaffrey *et al.* 2008). More recent inversions of CGPS displacements from slow slip events in the Gisborne area suggest that the downdip limit of slow slip could be further west, near the longitude of Gisborne. These events occur in an area where deep 8–12 s pre-stack time-migrated seismic reflection data are available, potentially capable of imaging structure to ∼15 km (previously described by Barker *et al.* 2009). We use these data to characterize the subduction interface in the offshore Gisborne area

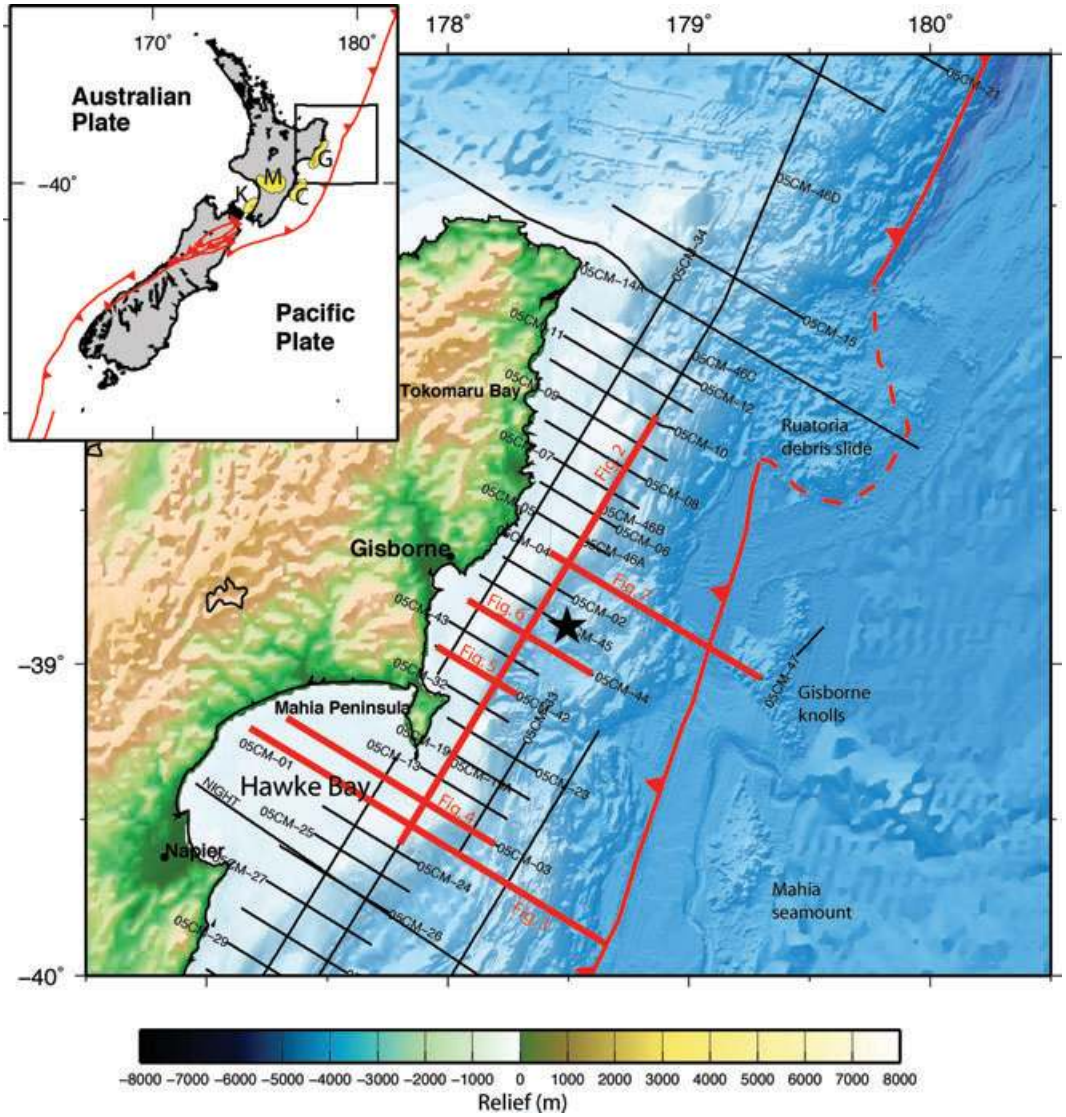

Figure 1. Location map of the east coast North Island study region offshore Gisborne. Black lines are locations of the 05CM seismic profiles described in the text. Topography and bathymetry are from ETOPO2 (Smith & Sandwell 1997) and swath bathymetry has been merged where available. Red toothed line is the approximate frontal thrust at the toe of the accretionary wedge and black star is the epicentre of the Mw 6.6 December 2007 normal-faulting earthquake within the subducted slab. Inset is a summary of New Zealand regional tectonics. Yellow patches indicate areas of the Hikurangi margin where slow slip has been recorded (McCaffrey *et al.* 2008). K = Kapiti, M = Manawatu, C = Cape Kidnappers and G = Gisborne slow slip events.

and identify geometrical and potentially compositional features that could explain the occurrence of slow slip here. There is a need to better understand this part of the margin that experiences repeated slow slip events to assess its significance on stress accumulation and its seismic risk to Gisborne.

3 DATA AND METHODOLOGY

3.1 05CM survey seismic reflection data

This study uses seismic reflection data from the 05CM survey conducted by Crown Minerals (New Zealand's Ministry for Economic Development) and GNS Science in May 2005 (Barker *et al.* 2009). This survey consisted of ca. 2800 km of 2-D seismic reflection data made up of 33 dip profiles and six strike profiles. These data were acquired by Multiwave Geophysical (Multiwave 2005) onboard MV Pacific Titan using a 4140 cubic inch, 2000 p.s.i. air gun source. Streamer length varied in the survey from 12 to 4 km due to shark attacks destroying the streamer. Record lengths varied from 8 to 12 s, depending on streamer length and shot intervals were 37.5 and 25 m for different lines. These data were processed by GNS Science and Fugro Seismic Imaging and pre-stack time migrated with 12.5 m common depth point (CDP) bins (Multiwave 2005). The data set is also supplemented by the NIGHT seismic profile described by Henrys *et al.* (2006).

3.2 Velocity analysis and depth conversion

Depth conversion of interpretations in this study follows the velocity analysis and time–depth models outlined for these data by Barker *et al.* (2009). Barker *et al*. (2009) apply the Dix equation to stacking velocities, derived from normal moveout (NMO)

corrections of CDP gathers to derive time–depth relations (Barker *et al*. 2009; their Fig. 8) and compare them with the detailed velocity analyses from wide-angle arrivals and pre-stack depth migration from the NIGHT line (Henrys *et al.* 2006). Seismic velocities were determined at 500 m intervals along each line. Over the depth range we are interested in for interpreting the interface (∼6–12 s), the mean velocity model implies an average velocity of ca. 4.5 km s^{-1} at a depth of 6 km below the seafloor (with a 0.5 km standard deviation in depth) and ca. 6 km s^{-1} at 15 km (with a 1.0 km standard deviation in depth) (Barker *et al.* 2009; their Fig. 9).

4 SEISMIC REFLECTION CHARACTER OF THE SUBDUCTION INTERFACE OFFSHORE GISBORNE

The term subduction interface used here describes the boundary between the subducting oceanic crust (and any underthrust material) and the deformed overriding plate and accretionary wedge. Here we investigate in detail the geometry and reflection characteristics of this interface in the region from northern Hawke Bay to Tokomaru Bay, in the general vicinity of the observed slow slip events (Fig. 1). This region has also been highlighted by Barker *et al.* (2009) as an area of increased subduction thrust roughness and complexity.

4.1 Northern Hawke Bay to Mahia Peninsula

To the south of Mahia Peninsula (lines 05CM-01 to -19, also crossed by strike-line 05CM-46; Figs 2, 3 and 4), the subduction interface is interpreted as a surface that separates the poorly reflective base of the overlying plate from downgoing material with high-amplitude reflectivity (Fig. 4). Splay faults within the overriding plate sole out onto this surface in the east (Fig. 4). Line 05CM-01, which extends further east and west than 05CM-03 shows that these high-amplitude reflections fade out against an unreflective part of the downgoing plate to the east and diminish in amplitude to the west (Fig. 3). The distinctive high-amplitude reflection character occurs beneath the interface between depths of 7–16 km, and is also imaged on the margin-parallel strike-line 05CM-46 (Fig. 2). We name this zone of distinctive seismic reflectivity the high-amplitude reflectivity zone-1 (or HRZ-1).

Depth conversion of the interface geometry on line 05CM-01 reveals that west of CDP 10000 the interface dips smoothly landward at ∼8° until a depth of ∼10 km at CDP 6000. At CDP 6000, the interface takes a steep step downwards to a deeper level of ∼15 km and then continues to dip westwards at ∼8° (Fig. 3c). The interface dips seaward to the east of CDP 10000.

Seismicity, as recorded and located by the GeoNet network (www.geonet.org.nz), is concentrated below a depth of 22 km with a marked updip limit of seismicity (Figs 3c and 4c). The majority of seismicity lies more than ∼4 km below the interface, although there are a few events (notably two M_L 4–6 events) located on the interface itself. The only significant seismicity within the overriding plate occurs in the vicinity of interpreted splay faults, suggesting that these are presently active structures (Figs 3c and 4c). We note here, however, that depth errors in the GeoNet locations for offshore earthquakes are likely of the order ±5 km due to the fact that only land seismograph stations are available and the assumption of a horizontal-layer velocity model for location, which does not fully account for the effect of dipping subduction crust. Horizontal positions are much better constrained.

4.2 Mahia Peninsula to Gisborne

The distinctive HRZ-1 reflection character that was observed below parts of the interface on lines 05CM-01 to -19 is not observed beneath the interface between Mahia Peninsula and Gisborne on lines 05CM-23 to -45 (Fig. 1). On lines 05CM-42 and -43, a distinction between low-amplitude reflections of the overlying wedge and a higher amplitude reflectivity subducting plate can be interpreted at ∼6 s two-way traveltime, but the distinction is not as clear as that observed on lines 05CM-01 and -03 (Figs 3 and 4). East of CDP 1000, line 05CM-42 between 4 and 6s two-way traveltime there are two high-amplitude reflections, either of which could be interpreted as the subduction interface (Fig. 5). To the west, these horizons can be less confidently interpreted and they eventually merge in a zone of high-amplitude reflectivity. Between these high-amplitude reflections is a lens of lower amplitude material. The probable complex structure of the interface in this area makes a confident interpretation with 2-D seismic data difficult. However, the interpretation of a lens of lower amplitude reflectivity on other dip-lines in the region and on the strike-line 05CM-46 (Fig. 2) suggests it is a real feature. When the extent of this seismic character is mapped in plan view it has a diameter of 20–30 km and the lens of material between the two high-amplitude reflections reaches a maximum thickness of ∼1.5 km. We name this zone of distinctive seismic reflectivity the lens reflectivity zone (LRZ).

Immediately offshore Gisborne, on line 05CM-44 (Fig. 6), the subduction interface is again more clearly identified as the transition from low-amplitude overriding plate reflections to higher-amplitude reflections of the lower plate. However, seismic reflection character below the subduction interface in Fig. 6 does not consist of the same high-amplitude, parallel and continuous reflectors as those observed beneath the interface in the region of the HRZ-1 (Figs 3 and 4). The subduction interface on line 05CM-44 is relatively smoothly dipping landward at ∼8–10°. Around CDP 3500 two high-amplitude interface reflections are observed (Fig. 6). These reflections may be the result of the complex lens geometry feature (LRZ) also interpreted on lines further south (Fig. 5).

Seismicity on lines 05CM-32 to -44 is concentrated below the subduction interface and landwards of the potential LRZ (see Figs 5c and 6c).

4.3 North of Gisborne to Tokomaru Bay

Between Gisborne and Tokomaru Bay, the subduction interface has a variable geometry and reflection character, and differs to that seen between Mahia and Gisborne (Fig. 7). The interface is very well imaged as a single high-amplitude reflection east of line 05CM-04 CDP 3500 (Fig. 7). This high-amplitude reflection separates the narrow accretionary wedge from a poorly reflective subducting plate. A number of splay faults and the frontal thrust sole out onto this surface.

Between line 05CM-04 CDP 2000 and 3500, the interface is more difficult to interpret as reflections at ∼4.5 s two-way traveltime are all of similar amplitude (Fig. 7b). A high-amplitude seaward dipping reflection within the underlying plate potentially exists around CDP 3500, ∼5–7 s two-way traveltime (Fig. 7b). The interface is well defined west of line 05CM-04 CDP 2000 where it is interpreted as the uppermost reflection of a 1.5–2 s two-way traveltime wide band of high-amplitude, parallel and continuous reflectivity. This reflectivity band becomes more discontinuous landward as the interface deepens and reaches the bottom of the 8 s recording limit of line 05CM-05 (Fig. 7). We suggest the high-amplitude

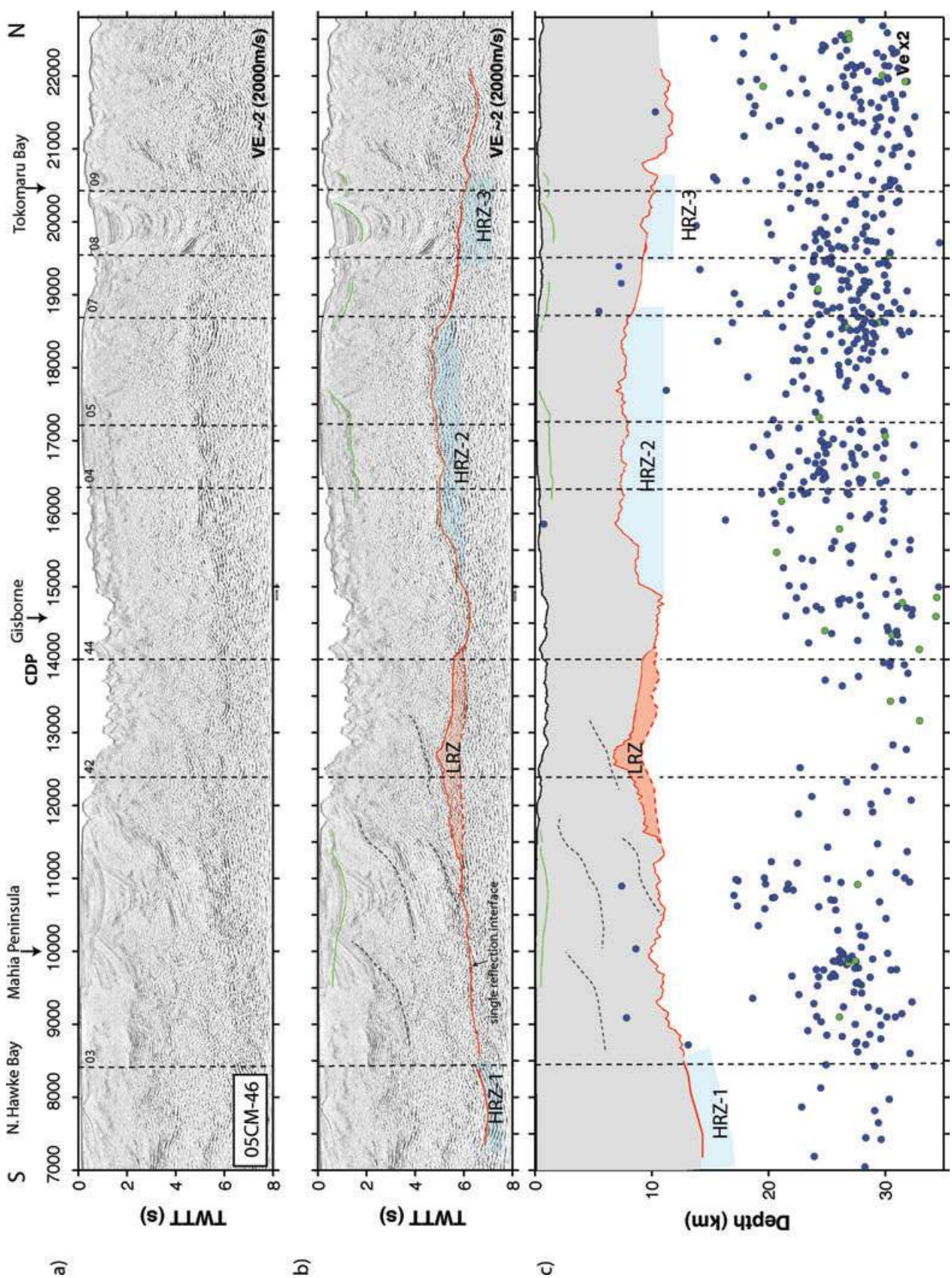

Figure 2. (a) Un-interpreted and (b) interpreted along-margin seismic profile 05CM-46 (Fig. 1). Red line is the subduction interface; green line is an unconformity within stratified sediments. Dotted lines are tie lines with other figures (Fig. 1). (c) Depth converted interpretation based on the velocity model described in Section 3.2. Vertical dotted lines are seismic-reflection tie lines and thinner dotted lines are interpreted splay faults. Seismic profile was acquired with an 8-km-long streamer. Blue dots are seismicity $<M_L$ 4, green dots M_L 4–6 and red dots $>M_L$ 6 between January 1990 and June 2008 within 10 km of the profile. Event locations were derived from the GeoNet catalogue (www.geonet.org.nz), filtered to remove events which lack adequate depth constraint.

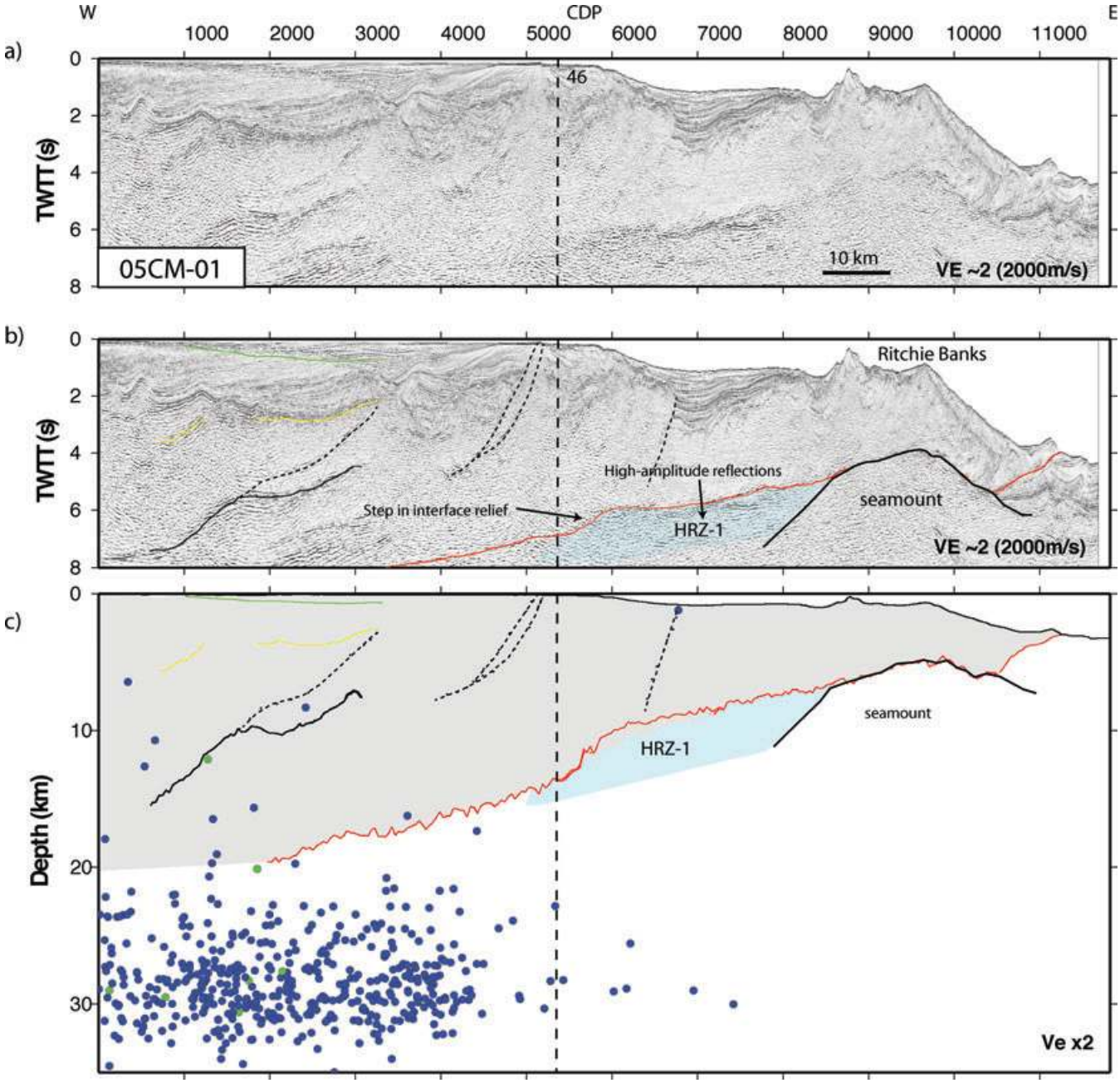

Figure 3. (a) Un-interpreted and (b) interpreted seismic profile 05CM-01 from northern Hawke Bay (Fig. 1). Red line is the subduction interface, yellow line is the base of well-stratified sediments, green line is an unconformity within stratified sediments. Dotted line is the intersection with along-strike profile 05CM-46 (Fig. 2). (c) Depth-converted interpretation based on the velocity model described in Section 3.2. Seismic profile was acquired with an 8-km-long streamer. Dots are seismicity as described in Fig. 2.

reflection character ceases around line 05CM-05 CDP 1000, although the poor data quality at this depth means it could continue even further to the west. This seismic character is very similar to that observed on 05CM-01 and is also imaged clearly on the strike-line 05CM-46 (Fig. 2). We name parts of the interface with this seismic character the HRZ-2.

The interface in this area, as well as showing variable reflection character, also varies in its geometry. At CDP 500, line 05CM-05, the interface is at a level of ∼12 km (Fig. 7c), similar to the depth of the interface at the equivalent distance from the trench on line 05CM-44 (Fig. 6c). However, between CDP 1000 and 2000, the interface takes a steep step upwards, and the interface at CDP 2000 is only ∼8 km deep. East of CDP 2000 on line 05CM-05, and CDP 500 on line 05CM-04, the interface dips smoothly at ∼4° (Fig. 7c). The effect of this step-up in interface geometry can also be observed on 05CM-46, where the interface becomes ∼3 km shallower than its usual depth for an along-margin distance of 50 km (Fig. 2c). The high-amplitude reflection character, given the limitations in the quality of our data towards the ∼8 s threshold of recording, appears to fade out westward at a location corresponding with the step-up in interface relief, as was the case for the HRZ-1 along line 05CM-01 (Fig. 3). The along-margin strike-line

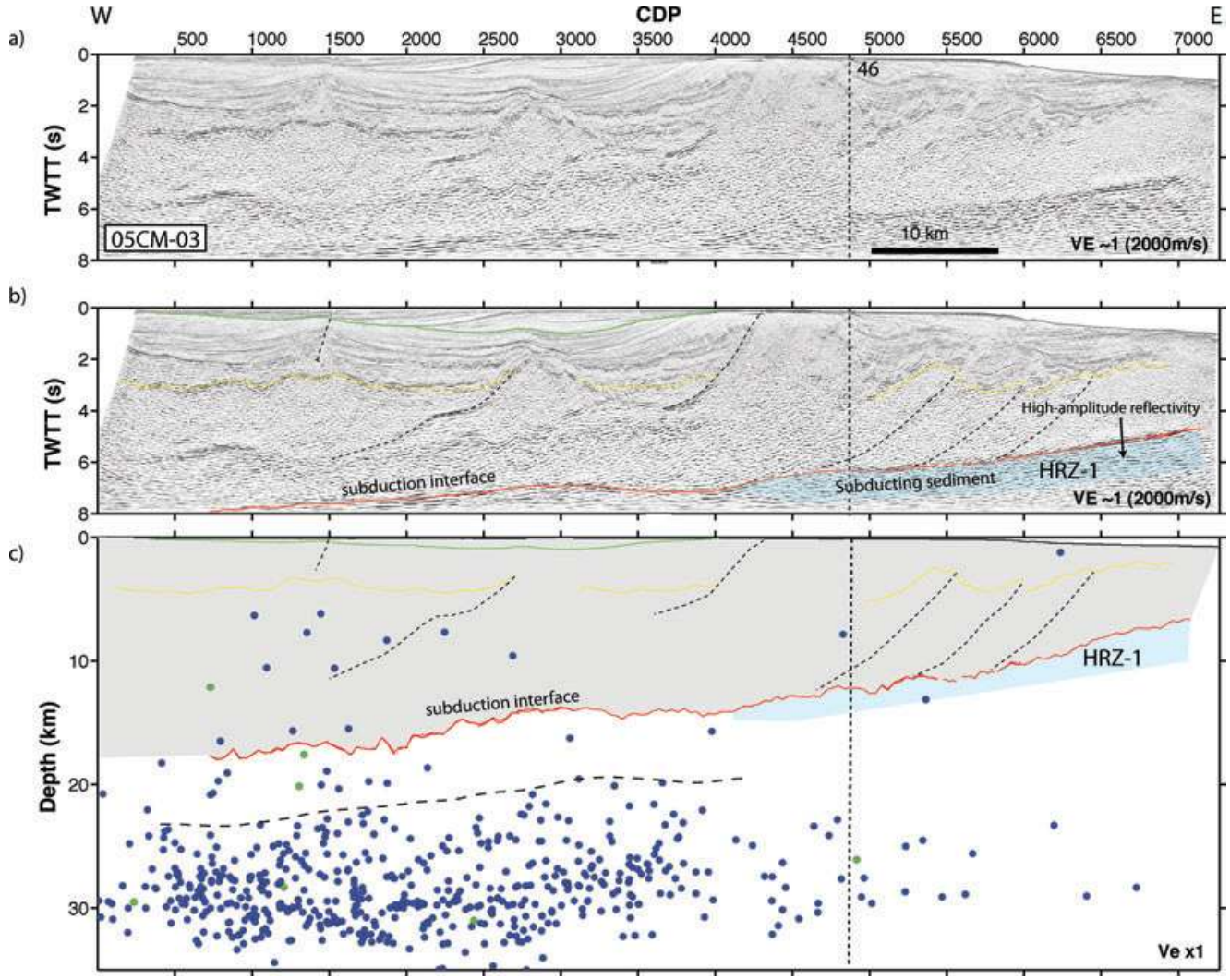

Figure 4. (a) Un-interpreted and (b) interpreted seismic profile 05CM-03 from northern Hawke Bay (Fig. 1). Red line is the subduction interface, yellow line is the base of well-stratified sediments, green line is an unconformity within stratified sediments. Dotted line is the intersection with along-strike profile 05CM-46 (Fig. 2). (c) Depth-converted interpretation based on the velocity model described in Section 3.2. Seismic profile was acquired with an 8-km-long streamer. Dots are seismicity as described in Fig. 2.

05CM-46 shows that the occurrence of HRZ-2 reflection character correlates directly with the region of shallower interface relief (Fig. 2). High-amplitude reflectivity fades out eastwards on line 05CM-04 towards an unreflective part of the interface, analogous to the eastward end of the observed HRZ-1 reflection character on line 05CM-01 (Fig. 3).

HRZ-2 reflection character is not identified on line 05CM-07 (not shown here), where the subduction decollement deepens to a more usual depth of ∼12 km at the position of its crossover with line 05CM-46 (Fig. 2c). High-amplitude reflections are, however, identified again beneath parts of the interface on dip-lines 05CM-08 and -09 (not shown here) further north and the interface becomes locally shallower in these areas. We call this small patch of high-amplitude reflectivity the HRZ-3. North of Tokomaru Bay the subduction interface deepens further and approaches the maximum 8 s recording depth. Imaging of the interface here is poor due to its depth and the fact the seafloor is greatly disrupted by slope failure (Lewis *et al.* 2004; Barker *et al.* 2009).

There is significant intraslab seismicity beneath the HRZ-2, below a depth of ∼20 km. This seismicity includes a number of M_L 4–6 events (Fig. 7c). The updip limit of intraslab seismicity correlates generally with the updip limit of the HRZ-2, but there is no clear relationship between changes in intraslab seismicity and the downdip limit of the HRZ-2 reflection character (Fig. 7c). The December 2007 Mw 6.6 earthquake occurred at a depth of 40 km within the downgoing slab, below the southeast corner of interpreted HRZ-2 reflection character (Fig. 8).

5 DISCUSSION

5.1 Structure of the interface offshore Gisborne

Along the northeast Hikurangi margin we have identified and mapped three distinctly different types of interface seismic reflection character: (1) In three separate locations, we identify packages of well-defined, high-amplitude reflectivity below the interface up to 2 s thick (HRZ-1, -2 and -3; Figs 3, 4, 7 and 8); (2) Reflections with a potentially lens-shaped geometry exists above or below the interface offshore Gisborne (the LRZ), although the true geometry

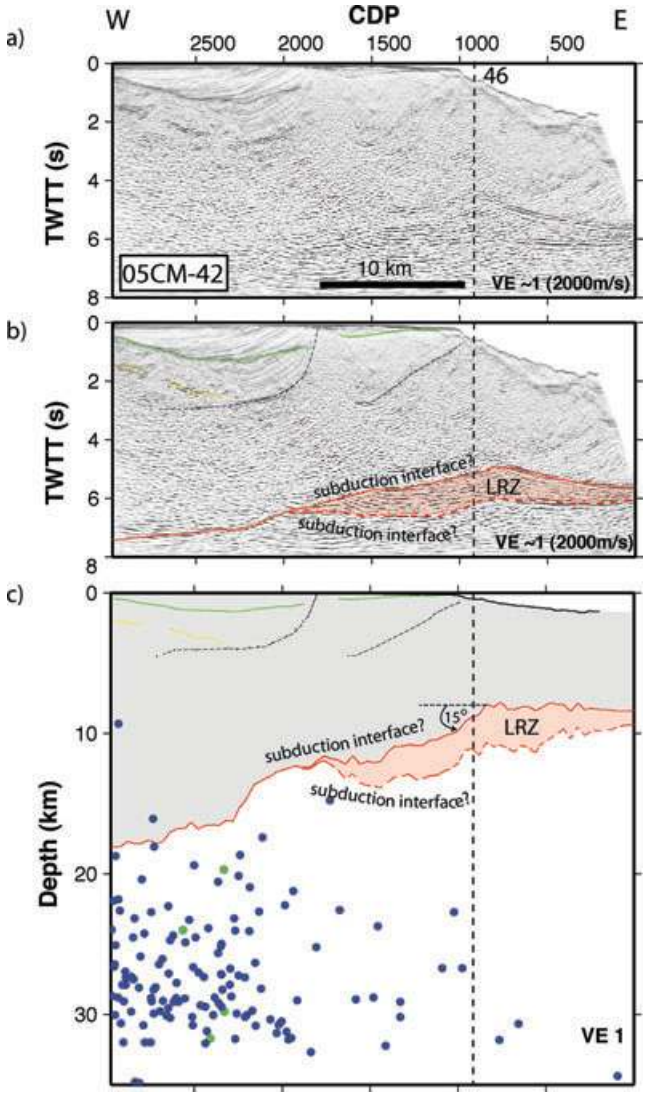

Figure 5. (a) Un-interpreted and (b) interpreted seismic profile 05CM-42 from north Mahia Peninsula (Fig. 1). Red line is the subduction interface, yellow line is the base of well-stratified sediments, green line is an unconformity within stratified sediments. Double headed arrows highlight orientation of reflections inside and outside the wedge. Dotted line is the intersection with along-strike profile 05CM-46 (Fig. 2). (c) Depth-converted interpretation based on the velocity model described in Section 3.2. Seismic profile was acquired with an 8-km-long streamer. Dots are seismicity as described in Fig. 2.

is difficult to identify with 2-D seismic data (Figs 5 and 8) and (3) In all other locations between northern Hawke Bay and Tokomaru Bay, the interface is more smoothly dipping with no well-defined, high-amplitude, parallel and continuous reflectivity beneath the interface (Fig. 6).

The high-amplitude reflections of the HRZ-1 and -2 are observed downdip of an unreflective portion of the interface (Figs 3 and 7). This unreflective region on line 05CM-01 corresponds to the area where a subducted seamount has been interpreted by Barker *et al.* (2009). The subduction of this seamount has deformed the outer wedge to produce an outer high, known as Ritchie Banks (Fig. 3). The location of this seamount interpreted from seismic profiles 05CM-01 (Fig. 3) and 05CM-33 (not shown here), also corresponds with an NNE–SSW striking magnetic anomaly of up to +280 nT (Fig. 8). The incoming Pacific Plate offshore Gisborne has a fairly low, uniform magnetic signature, with the only major anomalies > +150 nT (up to +550 nT), corresponding to un-subducted seamounts (e.g. the Mahia seamount and Gisborne Knolls; Fig. 8). We suggest the lower amplitude (up to +220 nT) magnetic anomaly to the west of the subduction front, in the area of the subducting seamount imaged on 05CM-01, is the result of the subduction of a seamount with a high positive magnetic anomaly, like those currently not yet subducted on the Pacific Plate. We suggest this magnetic anomaly can thus be used to roughly estimate the extent of the subducted seamount where it is not constrained by seismic data (cf. Barckhausen *et al.* 1998; Honkura *et al.* 1999; Fig. 8). Similarly, updip of the HRZ-2 on line 05CM-04, there is evidence for another subducted seamount (Fig. 7): a seaward-dipping reflection exists within the underlying plate, which could be associated with a seaward-dipping seamount flank; an uplifted ridge in bathymetry above the unreflective interface is likely the result of seamount subduction; and another NE–SW striking +280 nT magnetic anomaly corresponds with this region where we suspect a subducted seamount from seismic reflection data (Fig. 8).

Although seismic profiles defining the third shallow HRZ-3 do not extend far enough east to image the termination of this reflection character, the possibility that a seamount has also been subducted in this area is supported by yet another +250 nT magnetic anomaly (Fig. 8). Elsewhere to the west of the deformation front from northern Hawke Bay to Tokomaru Bay, there are no other magnetic anomalies above +150 nT.

The HRZ seismic reflection character in all cases is interpreted downdip of observed or inferred subducted seafloor topography (Fig. 8). We suggest that these high-amplitude reflections result from sediments (probably turbidites) and eroded overriding plate material, which have been underthrust as the decollement is forced upwards to accommodate the subducting topography (e.g. Lallemand *et al.* 1994; Bangs *et al.* 2006). The brightness of seismic reflections seen in the HRZ areas may suggest that the underthrust sediments are fluid-rich and/or contain varying sand contents, creating a large impedance contrast, similar to fluid-rich lenses associated with subducted seamounts along the central Ecuador margin (Sage *et al.* 2006). It could be argued that an alternative explanation for the reflection character could be that they are older underplated sediments. However, given the close association of this reflection character with seamounts, we favour that they are recently subducted sediments that have been entrained (e.g. Bangs *et al.* 2006). We also note from our structural mapping that in areas of HRZ reflection character the interface is locally shallower than the adjacent interface, due the effects of interface warping over the incoming subducting seamounts forming 'corrugations' or 'crestlines' on the otherwise NW-dipping interface (Fig. 8).

The origin of the lens of lower amplitude reflections defined by high-amplitude top and bottom reflections observed offshore Gisborne, is unclear and is not immediately related to subducting ridge structures (Figs 5 and 8). It is similar in character to 'megalenses' on the interface of the Middle America margin, which are interpreted to be erosional blocks from the upper plate or sheared off seamounts (Ranero & von Huene 2000). However, its true geometry is not resolvable using the 2-D seismic data available.

We suggest that the interface offshore Gisborne has highly heterogenous material properties and geometry (Fig. 8). In regions of seamount subduction, we suggest sediments with thicknesses of up to 2–4 km have been entrained, given the thickness of the high-amplitude reflection band (Figs 3 and 7), whereas other areas of

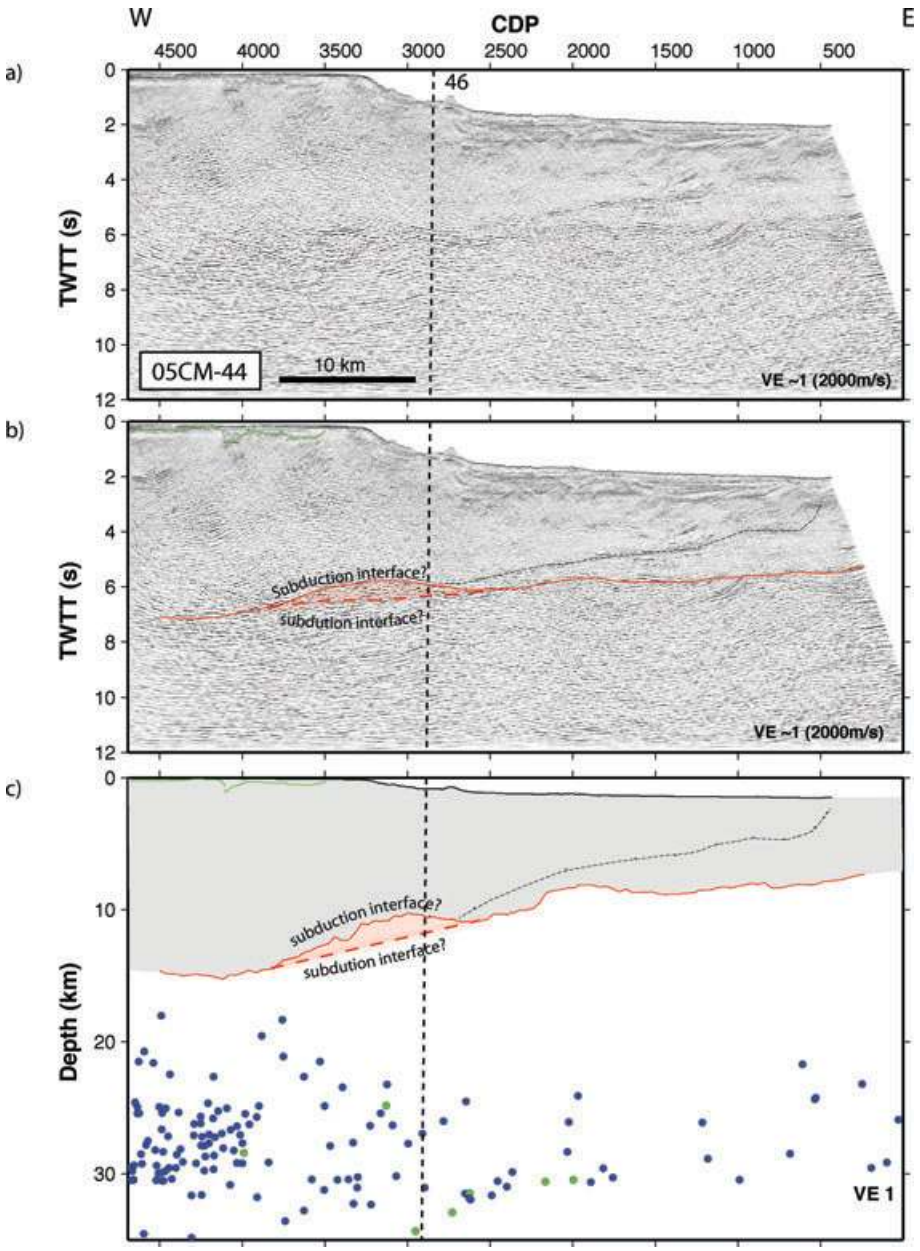

Figure 6. (a) Un-interpreted and (b) interpreted seismic profile 05CM-44 from offshore Gisborne. Red line is the subduction interface, green line is an unconformity within stratified sediments. Dotted line is the intersection with along-strike profile 05CM-46 (Fig. 2). (c) Depth-converted interpretation based on the velocity model described in Section 3.2. Seismic profile was acquired with a 12-km-long streamer. Dots are seismicity as described in Fig. 2.

the northeast Hikurangi margin within our study area show little evidence of underthrust sediments (e.g. Fig. 6). Our interpretation of variations in subducted sediment thickness supports converted seismic wave studies of the northeast Hikurangi margin by Eberhart-Phillips & Reyners (1999). These authors interpreted a generally 1- to 2-km-thick low-velocity zone beneath the interface that is up to 5 km thick in localized areas, at depths of 15–20 km. They inferred that this velocity structure represents a variable thickness subducting channel with near-lithostatic fluid pressures. Our study has mapped such sediment thickness variations in detail at depths of $<$15 km. The study by Eberhart-Phillips & Reyners (1999) suggests that the variations we have mapped in this study persist to deeper depths along the subduction channel.

5.2 Relationship between subduction interface character and slow slip

Slip distribution on the subduction interface in the slow slip events has been determined using estimated surface displacements from the events at CGPS sites in the region that are part of the NZ GeoNet network (www.geonet.org.nz). The start and end times of the slow slip events are estimated by eye from the time series, and the magnitudes of the time-series components at the start and end times are then picked automatically, and reviewed manually. The CGPS site displacements are calculated by differencing the picks between the start and end of the event, allowing for the steady interevent velocity.

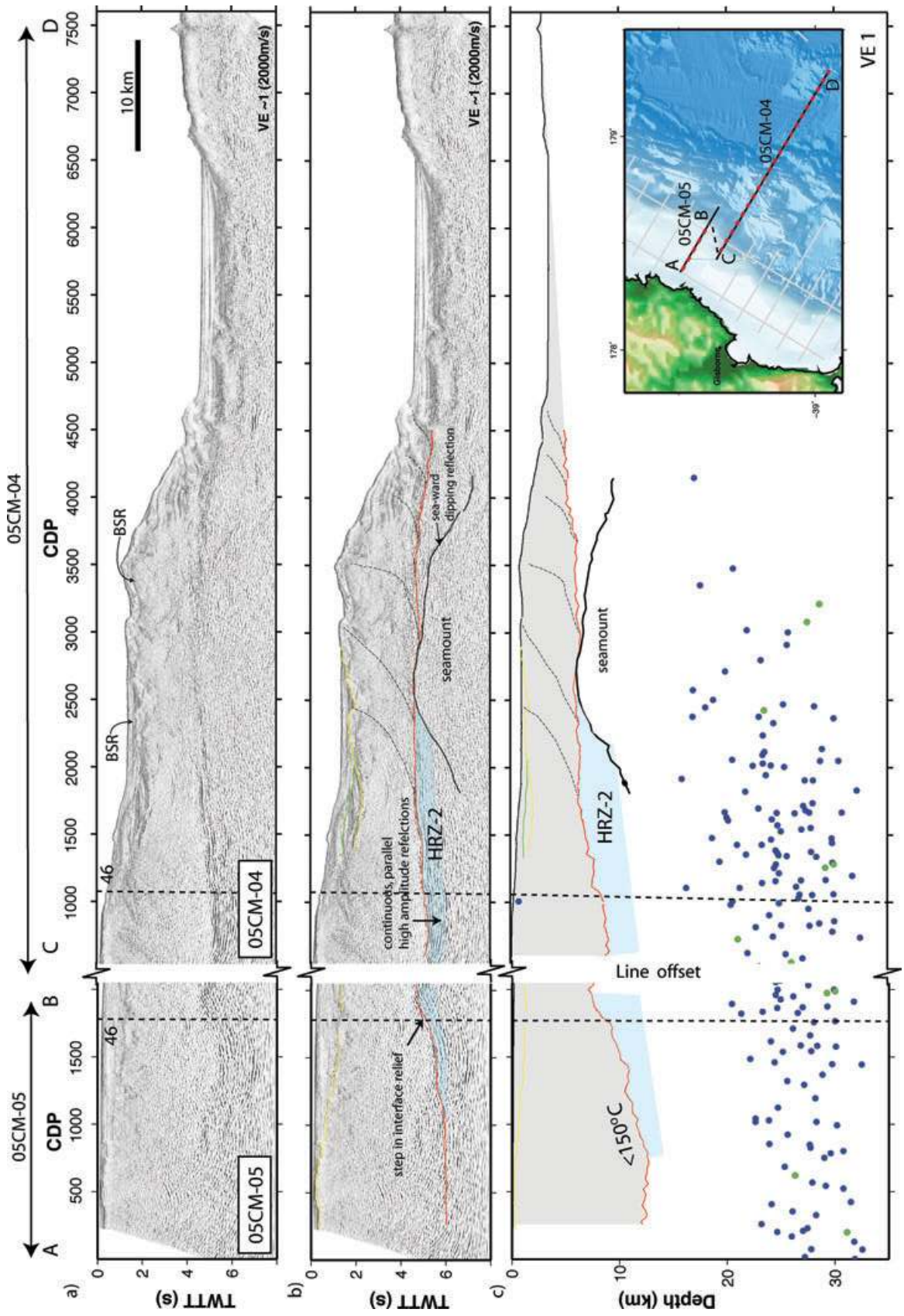

Figure 7. (a) Un-interpreted and (b) interpreted composite of seismic profiles 05CM-04 and -05 from north of Gisborne, linked together in the way described in the inset location map (red dotted line joining letters A–D). Red line is the subduction interface, yellow line is the base of well-stratified sediments and green line is an unconformity within stratified sediments. Dotted line is the intersection with along-strike profile 05CM-46 (Fig. 2). (c) Depth-converted interpretation based on the velocity model described in Section 3.2. Seismic profiles 05CM-04 and -05 were acquired with 12- and 8-km-long streamers, respectively. Dots are seismicity as described in Fig. 2. Conductive heat flow derived from BSR (bottom-simulating reflector) picks on 05CM-04, above the HRZ-2, is 32 ± 5 mWm^{-2} and thermal advection modelling (Molnar & England 1995) confirm that temperatures on the subduction thrust are <150°C along this part of the margin (see also McCaffrey *et al.* 2008).

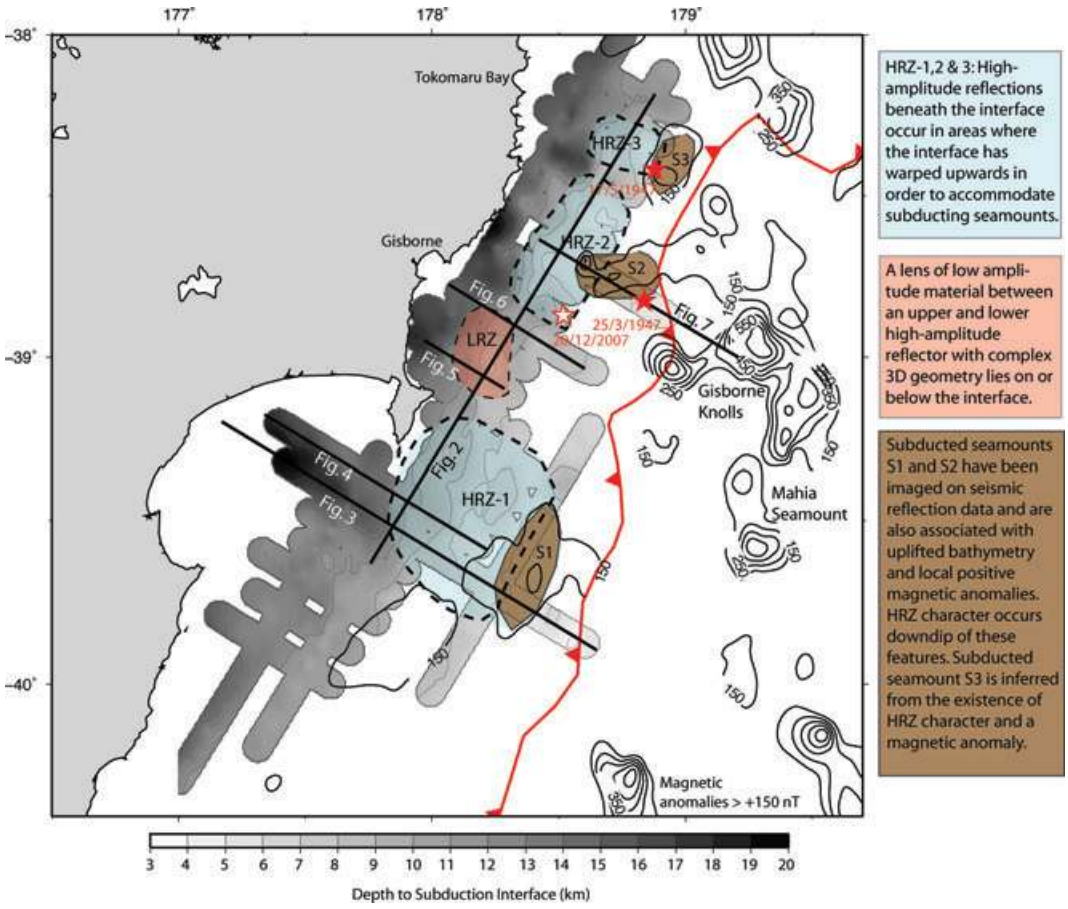

Figure 8. Interpreted depth to the subduction interface, following Barker *et al.* (2009), together with the locations of mapped interface seismic characteristics (coloured patches). Red stars show the locations of the 1947 tsunami earthquakes from Doser & Webb (2003) and the white star is the location of the Mw 6.6 intraplate earthquake in 2007. Magnetic anomaly data (bold contours) is plotted to show anomalies greater than +150 nT from Sutherland (1996), at a contour interval of 100 nT. Light contours are depth to subduction interface, with a contour interval of 2 km.

We invert the horizontal and vertical displacements at the CGPS sites for slip on the subduction interface during each slow slip event, using an inversion program (DEFNODE; McCaffrey 1995, 2002) to estimate coseismic displacements due to dislocations in an elastic half-space (Okada 1985). Rather than explicitly solving for the amount of slip at each of the nodes or patches defining the interface, we invert for three parameters describing a Gaussian function along separate downdip profiles of nodes (spaced at ∼50 km intervals along-strike) to estimate the depth and magnitude of the maximum slip and the spread of the slip (see also Subarya *et al.* 2006; Wallace & Beavan 2006 and http://www.rpi.edu/∼mccafr/defnode/defnode_071025.html for further description of the use of this approach to parameterize slip in DEFNODE). For the slow slip events discussed here, we estimated Gaussian parameters at two to four downdip profiles, depending on the along-strike distribution of CGPS data available during the event.

The modelled depth at which slow slip events occur along the northeast margin subduction interface (∼10–15 km) correlates with the depths at which we interpret localized thick underthrust sediments (the HRZ-1, -2 and -3) and shallower interface topography due to seamount subduction (Figs 9a to e). The interpreted interface lens of reflectivity seems to be a focus for slow slip and coincides with modelled locations of maximum slip for slow slip events in 2002, 2004 and 2006 (Figs 9a, b and c). The northernmost limit of interpreted interface high-amplitude reflection character (the HRZ-3) coincides with the location of the most northerly slow slip event detected to date (Fig. 9d). However, the resolution of the subduction interface north of the HRZ-3 is poor, which prevents confident interpretation that no further high-amplitude reflectivity exists there.

Although significant uncertainty remains both in the inversion of slow slip events and in our structural mapping due to data limitations, we propose that a general correlation exists between locations of slow slip and areas of the interface which have experienced locally thicker sediment subduction and shallower interface geometry due to subducting seamounts.

5.3 Slow slip mechanism in relation to interface structure in the Gisborne area

The spontaneous generation of slow slip events in regions of unstable to stable transitional frictional properties for certain effective stresses has been observed in laboratory experiments (Yoshida & Kato 2003) and in numerical rate-and-state friction law models (e.g. Shibazaki & Iio 2003; Liu & Rice 2007; Rubin 2008). Whether a fault experiences unstable or stable slip depends on the critical stiffness of the fault, $k_c = -(a-b)\sigma'/L_c$, where $(a-b)$ is the velocity dependence of the steady-state friction, σ' is the effective stress (normal stress minus pore fluid pressure) and L_c is a critical slip

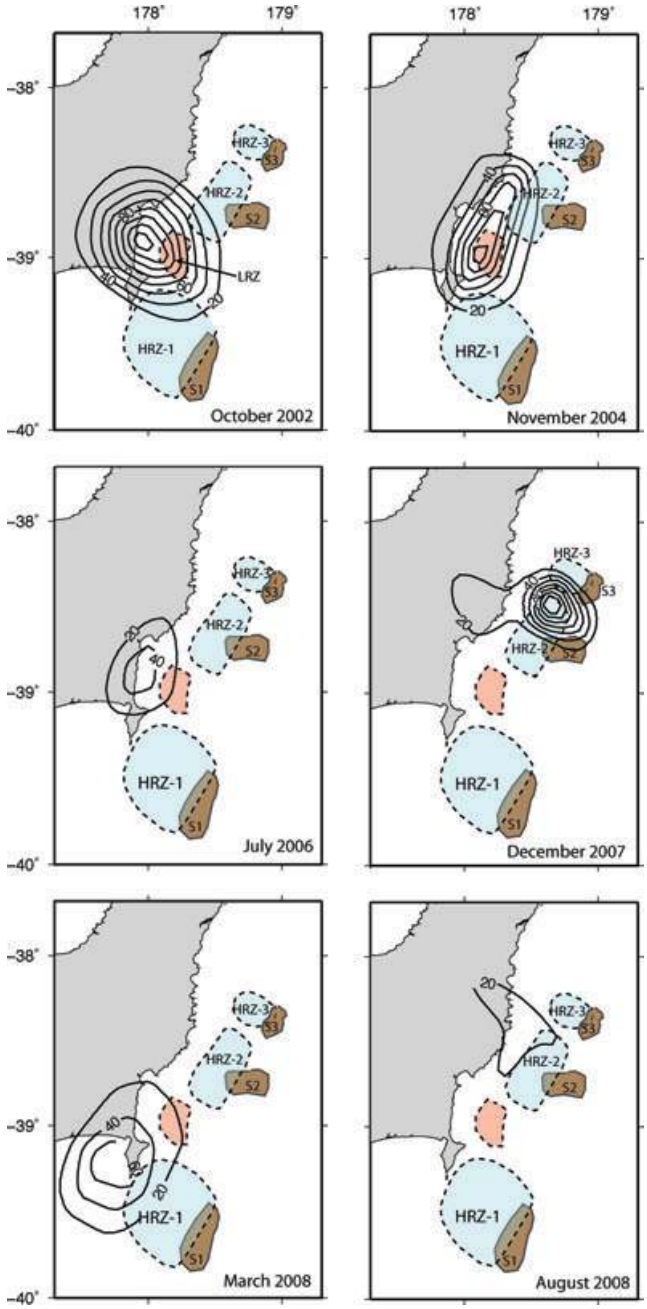

Figure 9. Comparison of mapped interface seismic characteristics with geodetically modelled slip magnitude distribution for slow slip events in 2002–2008. In (a)–(f), we invert CGPS displacements for three parameters describing a Gaussian function of slip amplitude along separate downdip profiles of nodes on the subduction interface (spaced at ∼50 km intervals along-strike); slip is interpolated for the rest of the interface between the profiles (see Section 5.2). Contours show the total slip on the interface in millimetre derived from the geodetic inversion.

distance (Ruina 1983; Scholz 1998). When $(a - b)$ is positive, the surface is steady-state velocity strengthening and stable slip occurs ($k_c < 0$). When $(a - b)$ is negative, the surface is steady-state velocity weakening and unstable slip occurs if $k < k_c$. At neutral stability, $k \approx k_c$, the system undergoes periodic oscillations in a conditionally stable regime (Ruina 1983; Scholz 1998).

From the rate-and-state friction law, the range of depths over which conditionally stable conditions for slow slip can occur is very narrow and does not explain why slow slip events are so common at many subduction margins (Rubin 2008). To increase the size range of slow slip events, high fluid pressures around the frictional transition zone that reduce effective stress have been suggested (Liu & Rice 2007). Liu & Rice (2007) have reproduced the ∼1-year periodicity of slow slip on a section of the Cascadia margin by assuming a near lithostatic pore pressure on the interface. Dilatancy is also believed to be a factor that can stabilize slow slip over wider areas (Segall & Rubin 2007; Liu *et al.* 2008). A number of observations suggest high pore pressures are associated with slow slip source regions, including tomographic images of high *P*-wave/*S*-wave velocity ratios (Shelly *et al.* 2006) and seismic reflection data (Kodaira *et al.* 2004). In addition, some studies suggest variations in interface effective stress caused by heterogenous fault geometries can promote conditions for slow slip (Mitsui & Hirahara 2006).

Hence, the combination of laboratory experiments and observations from around the world has highlighted the importance of low effective stress, either promoted by fluid pressure or slab geometry, in the genesis of slow-slip events. Below we explore what effect the subducted sediments and interface relief we have interpreted along the northeast Hikurangi margin may have on overburden pressures ($\sigma 3$) and fluid overpressures compared to parts of the interface free of underthrust sediment and corrugations, to assess their effect on interface effective stress (Fig. 10).

5.3.1 Role of subducted sediments

The role of subducted sediment on seismic coupling is a matter of much debate (Eberhart-Phillips & Reyners 1999). If subducted sediments are present, near lithostatic fluid pressures can develop within them, reducing normal stress which potentially leads to conditionally stable conditions and possibly slow slip. Overpressured subducted sediments may be expected if the decollement is impermeable and convergence rates are fast, burying them quickly. This is the case for the northeast Hikurangi margin (Wallace *et al.*, submitted).

5.3.2 Effect of topography on fluid pathways

We suggest that interface topography in regions of underthrust sediment may play an important role in reducing normal stress. The interface in front of-and-above the subducted seamounts is 2–4 km shallower than the surrounding interface (Fig. 8), resulting in significantly less overburden in the region of subducted seamounts, reducing normal stress (Fig. 10).

We further speculate that the shallow interface geometry in the vicinity of subducted seamounts, which form second-order structural corrugations on the interface, may affect fluid flow (Fig. 10). The 3-D structure of the HRZ regions (Fig. 10), and potentially also the lens of interface reflectivity (Figs 5 and 8), may lead to an increase in fluid flux into areas of lower mean stress, analogous to gold-bearing vein systems (Ridley 1993; Mair *et al.* 2000). Channelized fluid flow along fold-related structural permeability (Cox *et al.* 1991; Sibson 2005) and thrust ramps (Duuring *et al.* 2001) has been suggested as the mechanism for the generation of large gold-bearing veins. Development of supralithostatic fluid pressures along culmination zones on anticlines in the Bendigo goldfield in Victoria, Australia, is thought to be the result of large-scale fluid migration patterns (Cox *et al.* 1991). A similar flow concentration mechanism may increase fluid overpressures along the crestlines of the HRZ and lens, further decreasing effective mean stress in

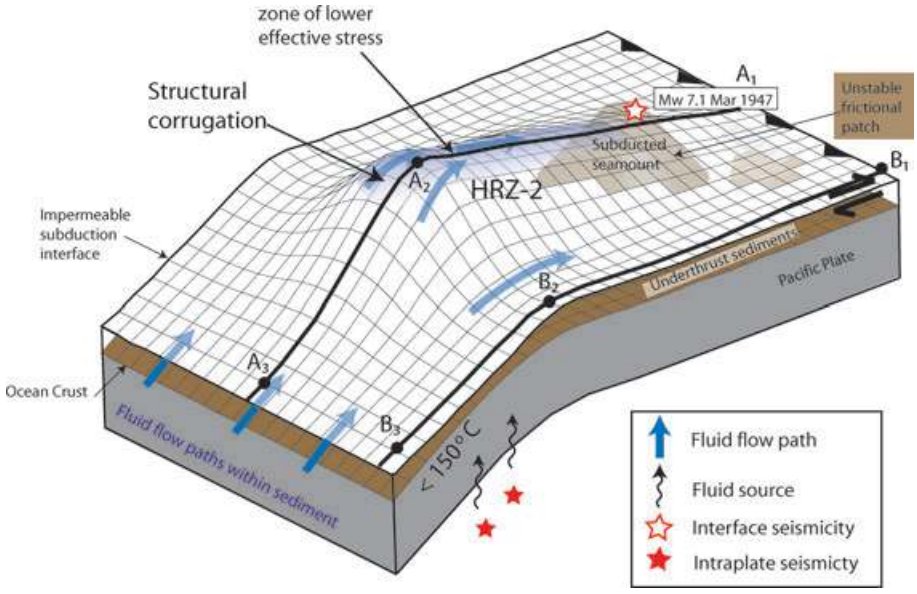

Figure 10. Schematic geometry of the subduction interface near HRZ-2 seismic-reflection character (Fig. 8). The interface has been warped upwards to accommodate the subduction of a seamount. We speculate that (1) the possibility of high overpressure within underthrusting sediments, (2) the smaller overburden stress above point A1–A2 compared to B1–B2 and (3) possible flow concentration effects along the crestline of the structural corrugation, result in low effective stress along this particular part of the interface.

these locations (Fig. 10). In addition, we may expect the presence of a less permeable seamount asperity to act as a blockage for fluid flow, leading to increased fluid overpressure and a low effective stress zone immediately in front of the seamount, which diverts flow around the blockage (Ridley 1993).

Therefore, we suggest that the interface offshore Gisborne may have a low effective mean stress due to the enhanced underthrusting of fluid-rich sediment, reduced overburden stresses where the interface has been warped to shallower depths to accommodate seamount subduction; and potential fluid flow concentration effects leading to overpressure along these shallower interface corrugations. We must caution, however, that this conceptual model is as yet untested, and we have no direct evidence of elevated fluid overpressures in the areas of slow slip.

However, in further support of this model is the fact that in March 1947 a tsunami earthquake occurred in the region of the subducted seamount updip of HRZ-2 reflection character (Fig. 8; Downes *et al.* 2000). Tsunami earthquakes have previously been correlated with regions of conditional stability likely caused by high fluid pressures (Bilek & Lay 2002; Seno 2002). We propose that the subducted seamount imaged on line 05CM-04 (Fig. 7) is effectively a stronger asperity within a region of low effective stress velocity-strengthening material (i.e. the HRZ-2) given the model described earlier. Rupture of this asperity into more stable frictional conditions can generate an earthquake with slow rupture velocity and long source–time duration, resulting in a large tsunami (Ito *et al.* 2007).

5.4 Comparison with other subduction margins

Slow slip events that have been recorded offshore Gisborne are on shallower parts of the subduction interface than have been recorded elsewhere in the world. Only one other comparable event is known to us, and it occurred in Costa Rica at a depth of 10–20 km (Protti *et al.* 2004); however, no detailed mapping of interface seismic characteristics in the region that slipped has been done to compare with the observations we present. The history of repeated slow slip events and tsunami earthquakes at shallow depths, combined with high-resolution seismic-reflection images of the subduction interface that slipped, make our study uniquely significant.

Globally, nearly all slow slip events are inferred to occur at depths of 30–45 km. The depth range and typical onshore setting results in much lower-resolution seismic-reflection images than we have available to us. However, even given this limitation, there are suggestions that broad-zones of high-amplitude reflections beneath the interface exist in zones of slow slip beneath the northern Cascadia (Nedimovic *et al.* 2003), Nankai trough (Kodaira *et al.* 2000) and Boso peninsula regions (Kimura *et al.* in press). Although we propose a mechanism for the generation of very shallow slow slip events and not these deeper events, the correlation of similar high-amplitude reflection zones in regions of deeper slow slip suggest there may be commonalities in the mechanism.

No shallow slow slip events have yet been detected along the southern Hikurangi margin (Fig. 1), however we do not have a comparable seismic-reflection data set in this area to investigate interface properties to make a comparison with the north margin. Despite that, however, we note some regional differences between the northern and southern margin that may be significant for future studies. The southern Hikurangi margin has a slower convergence rate ($<$30 mm yr^{-1} compared to 40–60 mm yr^{-1}) and a wider accretionary wedge than the northeast margin, and fewer seamounts are known on the incoming Pacific Plate than are observed farther north (Barker *et al.* 2009).

6 CONCLUSIONS

The interface reflection character and geometry at depths of 5–15 km, as interpreted from seismic-reflection data, is variable along the northeast Hikurangi margin between Mahia Peninsula and Tokomaru Bay. Three zones of high-amplitude interface

reflectivity (HRZ-1, -2 and -3) at depths of 5–15 km are interpreted to be the result of fluid-rich sediments that have been entrained adjacent to subducted seamounts. The interface above the HRZ zones is shallower by 2–4 km, as compared to the local average for an equivalent distance from the trench, and we interpret this as warping and the creation of a corrugation on the interface that accommodates seamount subduction.

We conclude that there is a general correlation between slow slip events in the Gisborne region and a subduction interface with high-amplitude seismic reflections that we interpret as fluid-rich subducted sediments. Further, the positions of discrete zones of high-amplitude reflectivity and shallower interface geometry correlate approximately with the best estimates for locations of slow slip from 2002 to 2008 and are downdip of the hypocenters of two tsunami earthquakes in 1947. We believe that to posit this spatial correlation is justified by the data, but acknowledge that the correlation requires further testing.

On the basis of the spatial correlations described earlier and our inference that high-amplitude seismic reflections near to the interface are associated with fluid-rich sediments, we hypothesise that effective stresses on the subduction interface may be lower in areas of high-amplitude reflectivity. The lower effective stress causes conditional stability that results in slow slip events and tsunami earthquakes. The primary factors we suggest that lead to conditional stability are: (1) the presence of fluid-rich sediment, (2) reduced overburden stresses (approximately normal to the interface) where the interface has been warped to shallower depths to accommodate seamount subduction and (3) hydrogeological effects of fluid flow concentration or blockage leading to enhanced overpressure along the crestlines of corrugations downdip from subducted seamounts.

ACKNOWLEDGMENTS

This research has been primarily funded by the New Zealand Foundation for Research, Science and Technology and the Ministry of Economic Development. The 05CM data set used in this study was acquired by Multiwave using the vessel Pacific Titan and was processed by GNS Science and Fugro Seismic Imaging. Claritas (GNS Science) seismic processing software and GMT (Wessel & Smith 1995) have been used in this study. Authors also thank Charles Williams and Bryan Davy for constructive comments on an earlier version of the paper. Authors also thank Reviewers Eli Silver and Nathan Bangs, and Editor Tim Minshull for constructive and useful comments.

REFERENCES

Bangs, N.L.B., Gulick, S.P.S. & Shipley, T.H., 2006. Seamount subduction erosion in the Nankai Trough and its potential impact on the seismogenic zone, *Geology,* **34,** 701–704.

Barckhausen, U., Roeser, H.A. & von Huene, R., 1998. Magnetic signature of upper plate structures and subducting seamounts at the cpnvergent margin off Costa Rica, *J. geophys. Res.,* **103,** 7079–7093.

Barker, D., Sutherland, R., Henrys, S. & Bannister, S., 2009. Geometry of the Hikurangi subduction thrust and upper plate, North Island, New Zealand, *Geochem. Geophys. Geosyst.,* **10,** Q02007, doi:10.1029/2008GC002153.

Bilek, S.L. & Lay, T., 2002. Tsunami earthquakes possibly widespread manifestations of frictional conditional stability, *Geophys. Res. Lett.,* **29**(14), doi:10.1029/2002GL015215.

Brown, K.M., Tryon, M.D., DeShon, H.R., Dorman, L.M. & Schwartz, S.Y., 2005. Correlated transient fluid pulsing and seismic tremor in the Costa Rica subduction zone, *Earth planet. Sci. Lett.,* **238,** 189–203.

Brudzinski, M.R. & Allen, R.M., 2007. Segmentation in episodic tremor and slip all along Cascadia, *Geology,* **35,** 907–910.

Calvert, A.J., 2004. Seismic reflection imaging of two megathrust shear zones in the northern Cascadia subduction zone, *Nature,* **428,** 163–167.

Cox, S.F., Wall, V.J., Etheridge, M.A. & Potter, T.F., 1991. Deformational and metamorphic processes in the formation of mesothermal vein-hosted gold deposits—Examples from the Lachlan fold belt in central Victoria, Australia, *Ore Geol. Rev.,* **6,** 391–423.

Delahaye, E.J., Townend, J., Reyners, M. & Rogers, G., 2009. Microseismicity but no tremor accompanying slow slip in the Hikurangi subduction zone, New Zealand, *Earth planet. Sci. Lett.,* **277,** 21–28.

Doser, D. & Webb, T.H., 2003. Source parameters of large historical (1917 to 1961) earthquakes, North Island, New Zealand, *Geophys. J. Int.,* **152,** 795–832.

Douglas, A., Beavan, J., Wallace, L.M. & Townend, J., 2005. Slow slip on the northern Hikurangi subduction interface, New Zealand, *Geophys. Res. Lett.,* **32,** LI6305, doi:10.1029/2005GL023607.

Downes, G.L., Webb, T.H., McSaveney, M., Darby, D., Doser, D., Chague-Goff, C. & Barnett, A., 2000. The March 25 and May 17 1947 Gisborne earthquuakes and tsunami: implication for tsunami hazard for east coast, North Island, New Zealand, in *Tsunami Risk Assessment Beyond 2000: Theory, Practice and Plans,* pp. 55–67, eds Gusiakov, V.K., Levin, B.W. & Yakovenko, O.I., Moscow.

Dragert, H., Wang, K. & James, T.S., 2001. A silent slip event on the deeper cascadia subduction interface, *Science,* **292,** 1525–1528.

Duuring, P., Hagemann, S.G. & Love, R.J., 2001. A thrust ramp model for gold mineralization at the Archean Trondhjemite-hosted Tarmoola deposit: The importance of heterogeneous stress distibutions around granitoid contacts, *Econ. Geol.,* **96,** 1379–1396.

Eberhart-Philips, D. & Reyners, M., 1999. Plate interface properties in the northeast Hikurangi subduction zone, New Zealand, from converted seismic waves, *Geophys. Res. Lett.,* **26,** 2565–2568.

Fagereng, A. & Ellis, S., 2009. On factors controlling the depth of interseismic coupling on the Hikurangi subduction interface, New Zealand, *Earth planet. Sci. Lett.,* **278,** 120–130.

Fisher, M., Brocher, T., Nokleberg, G., Plafker, G. & Smith, G., 1989. Seismic reflection images of the crust of the northern part of the Chugach Terrane, Alaska: Results of a survey for the Trans-Alaska Crustal Transect (TACT), *J. geophys. Res.,* **94**(B), 4424–4440.

Francois-Holden, C. *et al*., 2008. The MW 6.6 Gisborne earthquake of 2007: Preliminary records and general source characterisation, *Bull. New Zealand Soc. Earthq. Eng.,* **41,** 266–277.

Fujie, G., Kasahara, J., Hino, R., Sato, T., Shinohara, M. & Suyehiro, K., 2002. A significant relation between seismic activities and reflection intensities in the Japan Trench region, *Geophys. Res. Lett.,* **29**(7), 1100, doi:10.1029/2001GL013764.

Fukao, Y., 1979. Tsunami earthquakes and subduction processes near deep-sea trenches, *J. geophys. Res.,* **84,** 2303–2314.

Heki, K. & Kataoka, T., 2008. On the biannually repeating slow-slip events at the Ryukyu Trench, southwestern Japan, *J. geophys. Res.,* **113,** B11402, doi:10.1029/2008JB005739.

Henrys, S., Reyners, M., Pecher, I., Bannister, S., Nishimura, Y. & Maslen, G., 2006. Kinking of the subduction slab escalator normal faulting beneath the North Island of New Zealand, *Geology,* **34,** 777–780.

Hirose, H. & Obara, K., 2005. Repeating short- and long-term slow slip events with deep tremor activity around the Bungo channel region, southwest Japan, *Earth Planets Space,* **57,** 961–972.

Honkura, Y., Nagaya, Y. & Kuroki, H., 1999. Effects of seamounts on an interplate earthquake at the Suruga trough, Japan, *Earth Planets Space,* **51,** 449–454.

Ito, Y., Obara, K., Shiomi, K., Sekine, S. & Hirose, H., 2007. Slow earthquakes coincident with episodic tremors and slow slip events, *Science,* **315,** 503–506.

Kanamori, H., 1972. Mechanism of tsunamic earthquakes, *Phys. Earth planet. Inter.,* **6,** 346–359.

Kimura, H., Kasahara, K. & Takeda, T., in press. Subduction process of the Philippine Sea Plate off the Kanto district, central Japan, as

revealed by plate structure and repeating earthquakes, *Tectonophysics,* **472,** 18–27.

Kodaira, S., Takahashi, N., Nakanishi, A., Miura, S. & Kaneda, Y., 2000. Subducted seamount imaged in the rupture zone of the 1946 Nankaido earthquake, *Science,* **289,** 104–106.

Kodaira, S., Iidaka, T., Kato, A., Park, J.-O., Iwasaki, T. & Kaneda, Y., 2004. High pore fluid pressure may cause silent slip in the Nankai trough, *Science,* **304,** 1295–1298.

Lallemand, S.E., Schnurle, P. & Malavielle, J., 1994. Coulomb theory applied to accretionary and nonaccretionary wedges: possible causes for tectonic erosion and/or frontal accretion, *J. geophys. Res.,* **99,** 12 033–12 055.

Lewis, K.B., Lallemand, S. & Carter, L., 2004. Collapse in a Quaternary shelf basin off East Cape, New Zealand: evidence for passage of a subducted seamount inboard of the Ruatoria giant avalanche, *N. Z. J. Geol. Geophys.,* **47,** 417–429.

Linde, A.T. & Silver, P.G., 1989. Elevation changes and the great 1960 Chilean earthquake: support for asesimic slip, *Geophys. Res. Lett.,* **16,** 1305–1308.

Liu, Y. & Rice, R., 2007. Spontaneous and triggered aseismic deformation transients in a subduction fault model, *J. geophys. Res.,* **112,** B09404, doi:10.1029/2007JB004930.

Liu, Y., Rubin, A.M., Rice, J.R. & Segall, P., 2008. Role of fault dilatancy in subduction zone aseismic deformation transients and thrust earthquakes, *AGU Fall Meeting,* Abstract S34B-04.

Lowry, A.R., 2006. Resonant slow fault slip in subduction zones forced by climatic load stress, *Nature,* **442,** 802–805.

Mair, J.L., Ojala, J., Salier, B.P., Groves, D.I. & Brown, S.M., 2000. Application of stress mapping in cross-section to understand ore geometry, predicting ore zones and development of drilling strategies, *Aust. J. Earth Sci.,* **47,** 895–912.

McCaffrey, R., 1995. *DEFNODE Users Guide,* Rensselaer Polytechnic Institute, Troy, New York.

McCaffrey, R., 2002. Crustal block rotations and plate coupling, in *Plate Boundary Zones,* pp. 100–122, eds Stein, S. & Freymueller, J.

McCaffrey, R., Wallace, L.M. & Beavan, J., 2008. Slow slip and frictional transition at low temperature at the Hikurangi subdcution zone, *Nat. Geosci.,* **1,** 316–320.

McCausland, W., Malone, S. & Johnson, D., 2005. Temporal and spatial occurrence of deep non-volcanic tremor: from Washington to northern California, *Geophys. Res. Lett.,* **32,** L24311, doi:10.1029/2005GL024349.

Mitsui, N. & Hirahara, K., 2006. Slow slip events controlled by the slab dip and its lateral change along a trench, *Earth planet. Sci. Lett.,* **245,** 344–358.

Mochizuki, K. *et al*., 2005. Intense PP reflections beneath the aseismic forearc slope of the Japan Trench subduction zone and its implication of aseismic slip subduction, *J. geophys. Res.,* **110,** B01302, doi:10.1029/2003JB002892.

Molnar, P. & England, P.C., 1995. Temperatures in zones of steady-state underthrusting of young oceanic lithosphere, *Earth planet. Sci. Lett.,* **131,** 57–70.

Multiwave, 2005. Seismic Survey, Offshore East Coast–North Island, New Zealand, *New Zealand Unpublished Openfile Petroleum Report,* **3136,** 1–280.

Nedimovic, M., Hyndman, R., Ramachandran, K. & Spence, G., 2003. Reflection signature of seismic and aseismic slip on the northern Cascadia interface, *Nature,* **424,** 416–420.

Obara, K., 2002. Nonvolcanic deep tremor associated with subduction in southwest Japan, *Science,* **296,** 1679–1681.

Obara, K. & Hirose, H., 2006. Non-volcanic deep low-frequency tremors accompanying slow slips in the southwest Japan subduction zone, *Tectonophysics,* **417,** 33–51.

Okada, Y., 1985. Surface deformation due to shear and tensile faults in a half-space, *Bull. seism. Soc. Am,* **75,** 1135–1154.

Ozawa, S., Murakami, M. & Tada, T., 2001. Time-dependednt inversion study of the slow thrust event in the Nankai trough subduction zone, southwestern Japan, *J. geophys. Res.,* **106,** 787–802.

Pelayo, A.M. & Wiens, D.A., 1992. Tsunami earthquakes, slow thrust-faulting events in the accretionary wedge, *J. geophys. Res.,* **97,** 15 321–15 337.

Protti, M. *et al*., 2004. A creep event on the shallow interface of the Nicoya Peninsula, Costa Rica Seismogenic Zone, in *American Geophysical Union, Fall Meeting 2004,* San Francisco.

Ranero, C.R. *et al*., 2008. Hydrogeological system of erosional convergent margins and its influence on tectonics and interplate seismogenesis, *Geochem. Geophys. Geosyst.,* **9,** Q03S04, doi:10.1029/2007GC001679.

Ranero, C.R. & von Huene, R., 2000. Subduction erosion along the Middle America convergent margin, *Nature,* **404,** 748–752.

Reyners, M., 1998. Plate coupling and the hazard of large subduction thrust earthquakes at the Hikurangi subduction zone, *N. Z. J. Geol. Geophys.,* **41,** 343–354.

Ridley, J., 1993. The relations between mean rock stress and fluid flow in the crust: with reference to vein- and lode-style gold deposits, *Ore Geol. Rev.,* **8,** 23–37.

Rubin, A.M., 2008. Episodic slow slip events and rate-and-state friction, *J. geophys. Res.,* **113,** B11414, doi:10.1029/2008JB005642.

Ruina, A., 1983. Slip instability and state variable friction laws, *J. geophys. Res.,* **88,** 10 359–10 370.

Sage, F., Collot, J. & Ranero, C.R., 2006. Interplate patchiness and subduction-erosion mechanisms: evidence from depth-migrated seismic images at the central Ecuador convergent margin, *Geology,* **32,** 997–1000.

Scholz, C.H., 1998. Earthquakes and friction laws, *Nature,* **391,** 37–42.

Schwartz, S.Y. & Rokosky, J.M., 2007. Slow slip events and seismic tremor at circum-Pacific subduction zones, *Rev. Geophys.,* **45,** RG3004, doi:10.1029/2006RG000208.

Segall, P. & Rubin, A.M., 2007. Dilatancy stabilization of frictional sliding as a mechanism for slow slip events, *Eos Trans. AGU,* **88**(52), Fall Meeting Supplement, Abstract T13F-08.

Seno, T., 2002. Tsunami earthquakes as transient phenomena, *Geophys. Res. Lett.,* **29**(10), 1419, doi:10.1029/2002GL014868.

Shelly, D.R., Beroza, G.C., Ide, S. & Nakamula, S., 2006. Low-frequency earthquakes in Shikoku, Japan, and their relationship to episodic tremor and slip, *Nature,* **442,** 188–191.

Shibazaki, B. & Iio, Y., 2003. On the physical mechanism of silent slip events along the deeper part of the seismogenic zone, *Geophys. Res. Lett.,* **30,** GL017047, doi:10.1029/2003GL017047.

Sibson, R.H., 2005. Hinge-parallel fluid flow in fold-thrust belts: how widespread?, *Proc. Geol. Assoc.,* **116,** 301–309.

Smith, W.H.F. & Sandwell, D.T., 1997. Global sea floor topography from satellite altimetry and ship depth soundings, *Science,* **301,** 630–633.

Subarya, C. *et al*., 2006. Plate-boundary deformation associated with the great Sumatra–Andaman earthquake, *Nature,* **440,** 46–51.

Sutherland, R., 1996. Magnetic anomalies in the New Zealand region, 1:4,000,000, in *Geophysical Map 9. Lower Hutt: Institute of Geological & Nuclear Sciences*.

Wallace, L.M. & Beavan, J., 2006. A large slow slip event on the central Hikurangi subduction interface beneath the Manawatu region, North Island, New Zealand, *Geophys. Res. Lett.,* **33,** L11301, doi:10.1029/2006GL026009.

Wallace, L.M., Beavan, J., McCaffrey, R. & Darby, D., 2004. Subduction zone coupling and tectonic block roatations in the North Island, New Zealand, *J. geophys. Res.,* **109,** B12406.

Wallace, L.M. *et al*., 2009. Characterizing the seismogenic zone of a major plate boundary subduction thrust: the Hikurangi Margin, New Zealand, *Geochem. Geophys. Geosyst.,* **10,** Q10006, doi:10.1029/2009GC002610.

Webb, T.H. & Anderson, H., 1998. Focal mechanisms of large earthquakes in the North Island of New Zealand: slip partitioning at an oblique active margin, *Geophys. J. Int.,* **134,** 40–86.

Wessel, P. & Smith, W.H.F., 1995. New version of the generic mapping tools released, *Eos Trans. AGU,* **76**(33), 329.

Yoshida, S. & Kato, N., 2003. Episodic aseismic slip in a two-degree-of-freedom block-spring model, *Geophys. Res. Lett.,* **30,** GL017439, doi:10.1029/2003GL017439.